occurs because the term T_L becomes equal to $-T_R$ at this point.

Although the physical assumptions of the problem are no longer valid at this large value of λ, the result deserves additional discussion. For this value of λ (termed λ_{cr}) the deformation of the wing is unbounded because γ (and thus δ_o) is infinite. This behavior is, in the classical sense, a static divergence instability and is referred to in Ref. 2 as "wing-aileron divergence." In that reference, the authors studied the problem with a small perturbation approach and utilized the Galerkin method to obtain the approximate value $\lambda_{cr} = 32$. The present result is seen to be an exact determination of this hypothetical instability.

It should be noted that the addition of the trimming device precludes the discovery, from these equations, of bending divergence of the sweptforward wing. The reader is cautioned, however, that only static equilibrium is being investigated here. An additional, separate analysis is necessary to study aeroelastic stability.

The antisymmetrical application of ailerons assures lateral static equilibrium and also causes a different bending moment distribution on each wing. However, at the wing centerline or root, the bending moment is continuous because of the roll equilibrium requirement. The bending moment at the wing centerline, about an axis perpendicular to the wing elastic axis, is found to be

$$M_r = (2p_0L^2)T_RT_L \tag{8}$$

Without aeroelastic effects the bending moment at the wing root, due to the uniform load p_o, would be $M_{rigid} = p_oL^2/2$. The magnification of the bending moment due to aeroelasticity may be defined as

$$M.F. = M_r/M_{\text{rigid}} = 4T_RT_L \tag{9}$$

Figure 2 shows the quantity $4T_RT_L$ plotted vs q^*. M.F. is found to be 1.332 at a value of q^* to one-half. M.F. rises dramatically thereafter.

Conclusions

It is important to draw attention to the idealizations, and therefore shortcomings, present in this study. First of all, in real aircraft, bending *and* torsion flexibility are present and are elastically coupled. More importantly, the lift (here represented by p_o) is not uniformly distributed over the wing span, nor is the span of constant chord. The presence of three-dimensional aerodynamic effects due to finite wing-body combination and a tapered, more flexible wing will most certainly modify the simplistic formulae presented here.

The significance of these results lies in the fact that they present, via a closed-form solution, the essential features of the aeroelastically induced roll moment on the oblique wing. The results show that, depending on the magnitude of the ratio $q^* = q/q_{Div}$, antisymmetrical aileron trim is necessary for lateral static equilibrium of an elastically symmetric wing. The wing root bending moment is adversely affected as q^* increases. Since p_o is proportional to a large fraction of the aircraft gross weight (this fraction is nearly equal to unity, even after aeroelastic effects on total lift are considered) one may also speculate on the additional demands upon control surfaces as q^* increases. Although more sophisticated analysis is in order, this phenomenon appears to be an additional design consideration for an oblique winged aircraft.

References

[1]Brunelle, E. and Jones, R. T., "Letters-to-the-editor Exchange," *Astronautics and Aeronautics*, Vol. 11, No. 6, June, 1973, p. 4.

[2]Weisshaar, T. A. and Ashley, H., "Static Aeroelasticity and the Flying Wing," *AIAA Journal of Aircraft*, Vol. 10, No. 10, Oct. 1973, pp. 586–594.

[3]Diederich, F. W. and Budiansky, B., "Divergence of Swept Wings," TN 1680, 1968, NACA, Langley Field, Hampton, Va.

[4]Diederich, F. W. and Foss, K. A., "Charts and Approximate Formulas for the Estimation of Aeroelastic Effects on the Loading of Swept and Unswept Wings," TN 2608, 1952, NACA, Langley Field, Hampton, Va.

[5]Bisplinghoff, R. and Ashley, H., *Principles of Aeroelasticity*, Wiley, New York, 1962, pp. 479–481.

Hypersonic Flow Over Blunted Slender Wedges

A. V. Murthy*
National Aeronautical Laboratory, Bangalore, India

THE problem of inviscid hypersonic flow over blunted wedges has received the attention of many investigators. Theoretically, two well-known methods of calculation are due to Cheng[1] and Chernyi.[2] An interesting feature of Cheng's analysis is the oscillatory approach in pressure and shock waveshape for long downstream distances. Earlier results of Chernyi did not exhibit any oscillatory behavior and its absence was suspected to be due to the inclusion of the kinetic energy term in the analysis.[3] However, it has been reported recently by Schnieder[4] that Chernyi's approach also predicts an oscillatory decay but the wavelength and amplitude of the oscillation are quite different. An alternative approach which gives a nonoscillatory decay was suggested by Stollery[5] for the case of viscous interaction on a concave surface. The method was later extended to the case of thin blunted wedges by Stollery et al.[6] They used the tangent wedge approximation, which gives the correct downstream limit, in place of the Newton-Busemann pressure law employed in Cheng's theory, and integrated the resulting equation numerically. The modified method suppressed oscillatory behavior and the results agreed with the method of characteristics downstream.

The purpose of this Note is to show that the results of Ref. 6 can be obtained in closed form for the pressure and shock waveshape by integrating the equations analytically.[7] Further, it is indicated that the estimates of the method near the leading edge can be improved by incorporating modifications suggested by Kemp[8] to account for the effects of γ (ratio of specific heats).

Analysis

The blunt leading edge introduces a strong entropy gradient in the downstream flow which significantly modifies the pressure and heat transfer on the afterbody. By an analysis of the flow within the entropy layer, Cheng obtains the pressure-area relation as

$$p_e(y_e - y_b)^\gamma = \text{constant} \tag{1}$$

Here y_b is the body shape, y_e the edge of the entropy layer, p_e the pressure (assumed constant across the entro-

Received January 2, 1974. The author would like to thank J. F. Clarke and J. L. Stollery, both of Cranfield Institute of Technology, for suggestions and discussions.

Index category: Supersonic and Hypersonic Flow.

*Scientist, Aerodynamics Division.

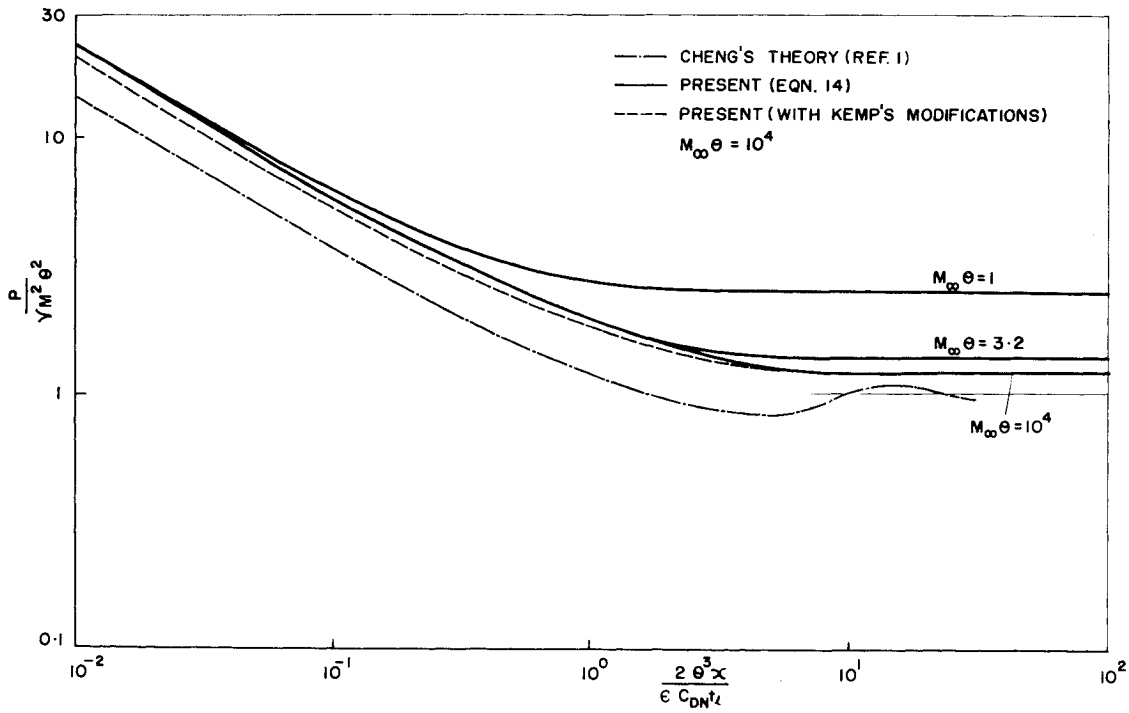

Fig. 1 Inviscid pressure distribution on blunted wedges ($\epsilon = \gamma - 1/\gamma + 1$).

py layer), and γ the ratio of specific heats. Equation (1) is further simplified by putting $\gamma = 1$ and evaluating the constant by considering the balance of momentum in the streamwise direction, as

$$p_e(y_e - y_b) = (\gamma - 1)/2 \cdot D_N \tag{2}$$

where D_N is the drag of the blunt nose. For a given body shape y_b, Eq. (2) along with a suitable pressure law determines the unknowns p_e and y_e. Considering the effective body surface to be described by y_e, according to the tangent wedge approximation pressure p_e is given by

$$P = \frac{p_e}{p_\infty} = 1 + \gamma(M_\infty y_e')^2\left[\frac{\gamma+1}{4} + \left\{\left(\frac{\gamma+1}{4}\right)^2 + \frac{1}{(M_\infty y_e')^2}\right\}^{1/2}\right] \tag{3}$$

where p_∞ = freestream pressure, M_∞ = freestream Mach number, and $y_e' = dy_e/dx$. For a slender blunt wedge of semiangle θ, $y_b = x\theta$ and by writing $X = x/L$, $Y_e = M_\infty y_e/L$ where L is a length scale, Eqs. (2) and (3) can be written as

$$P(Y_e - M_\infty\theta X) = K \tag{4}$$

and

$$(dy_e/dx) = (P-1)/\gamma\left[1 + \frac{\gamma+1}{2\gamma}(P-1)\right]^{1/2} \tag{5}$$

where

$$K = \frac{\gamma(\gamma-1)}{4} M_\infty{}^3 C_{DN}\frac{t_e}{L}$$

$C_{DN} = D_N/^{1/2}\rho_\infty U_\infty{}^2 t_e$, Leading edge drag coefficient

t_e = Leading edge thickness

Equations (4) and (5) are singular at the origin $X = 0$ and the solution valid near the leading edge is obtained by assuming $P = kX^m$ and determining m and k by substitution. Using this series solution valid near the leading edge, the equations were integrated numerically in Ref. 6. However, the equations can be integrated to give closed-form solution as shown below.

Substituting $t = Y_e - M_\infty\theta X$, and combining Eqs. (4) and (5), we get

$$dx = dt/F(t) \tag{6}$$

where

$$F(t) = \frac{(K/t - 1)}{\gamma\left[1 + \frac{\gamma+1}{2\gamma}(K/t-1)\right]^{1/2}} - M_\infty\theta \tag{7}$$

By integrating (6) from X_1 to X

$$X - X_1 = I(t) - I(t_1) \tag{8}$$

where

$$I(t) = \int\frac{dt}{F(t)} \tag{9}$$

Substituting

$$p^2 = 1 + \frac{\gamma+1}{2\gamma}\left(\frac{K}{t} - 1\right)$$

and splitting the integrand into partial fractions, $I(t)$ is written as

$$\frac{2(b_1 - b_0)}{\gamma+1} I = \int\left(\frac{b_1}{p-b_1} - \frac{b_0}{p-b_0}\right)\frac{dt}{dp}dp \tag{10}$$

$$= I_1(p, b_1) - I_1(p, b_0)$$

where

$$b_1 + b_0 = M_\infty\theta\frac{\gamma+1}{2}$$

$$b_1 b_0 = -1$$

$$I_1(p, b) = \int\frac{b}{p-b}\frac{dt}{dp}\,dp \tag{11}$$

After integration by parts, I_1 is obtained as

$$\frac{2\gamma}{\gamma+1}\frac{I_1(p,b)}{bk} = \frac{1}{(p-b)(p^2-a^2)} + \frac{1}{2a}[-E(p,a,b) + E(p,-a,b)] \tag{12}$$

where

$$a^2 = \frac{\gamma-1}{2\gamma} \tag{13a}$$

$$E(p, a, b) = \int \frac{dp}{(p+a)(p-b)^2} = \frac{1}{(a+b)^2} \ln\left(\frac{p+a}{p-b}\right) - \frac{1}{(a+b)(p-b)} \quad (13b)$$

Now, the integral $I(t)$ can be written as

$$I(t) = \frac{K(\gamma+1)^2}{4\gamma(b_1-b_0)}\left[\frac{b_1}{(p-b_1)(p^2-a^2)} - \frac{b_0}{(p-b_0)(p^2-a^2)} + \frac{b_1}{2a}\{E(p,-a,b_1) - E(p,a,b_1)\} - \frac{b_0}{2a}\{E(p,-a,b_0) - E(p,a,b_0)\}\right] \quad (14)$$

In particular, when the integration is from the blunt leading edge, the lower limits X_1 and t_1 in Eq. (8) are zero, and $X = I(t)$. The leading edge solution for $X \to 0$ is obtained by expanding Eq. (14) for $p \gg 1$ and the result for the pressure is

$$P(X \to 0) \approx [2/9 \cdot \gamma(\gamma+1)K^2]^{1/3} X^{-2/3}$$

Results and Discussions

The closed-form solution given by Eq. (14) was solved for different values of the incidence parameter $M_\infty \theta$ and the results are compared with Cheng's theory in Fig. 1. The values of X were obtained by calculating the integral I for different values of $P(= K/t)$. For each value of $M_\infty \theta$, there is a different downstream limit corresponding to the wedge value. Far downstream, Cheng's theory predicts an undershoot in pressure and a subsequent oscillatory approach to the downstream. Recently Cheng and Kirsch[9] have given a higher-order theory which almost removes the undershoot and predicts close agreement with the wedge value downstream.

Since the pressure area relation Eq. (2) is valid only in the limit of $\gamma \to 1$, in order to give good agreement with experimental results, Kemp suggested the following modification to Cheng's pressure area relation (Eq. 2)

$$p_e [y_s - (\gamma+1)/2 \cdot y_b] = (\gamma-1)/2 \cdot D_N \quad (15)$$

where y_s is the shock waveshape. When the leading edge is sharp, Eq. (15) reduces to the oblique shock theory result $y_s = (\gamma+1)2 \cdot y_b$ for $M_\infty \gg 1$. For the case of blunt leading edge, to use tangent wedge approximation along with Eq. (15), we need one more relation between y_s and the effective body shape y_e. For large M_∞, it is reasonable to assume $(\gamma+1)/2 \cdot y_e$ and the dotted line in Fig. 1 shows the results with these modifications.

For large $M_\infty \theta$, the solution can be obtained in a simpler form than Eq. (14) by approximating the tangent wedge rule as $P = (\gamma+1)/2 \cdot M_\infty{}^2 \theta^2$. This gives after integration the closed-form solution for the pressure

$$-(\gamma+1)/4 \cdot \zeta = \lambda + (\lambda^2/2) + \ln(1-\lambda) \quad (16)$$

$$\zeta = \frac{4\theta^3 X}{(\gamma-1)C_{DN} t_e}$$

$$\lambda = \left(\frac{\gamma+1}{2} \cdot \frac{\gamma M_\infty{}^2 \theta^2}{P}\right)^{1/2}$$

Though the solution (16) is valid for $M_\infty \theta \gg 1$, it is found to be quite accurate even for moderate values. For $M_\infty \theta = 1$ and $P = 28$, the values of $(2\theta^3 \kappa / \epsilon C_{DN} t_e)$ calculated by two Eqs. (14) and (16) differ only by 4%.

References

[1]Cheng, H. K., Hall, J. G., Golian, T. C., and Hertzberg, A., "Boundary-layer Displacement and Leading Edge Bluntness Effects in High Temperature Hypersonic Flows," *Journal of Aerospace Science*, Vol. 28, No. 5, May 1961, pp. 353–381.

[2]Chernyi, G. G., "Effect of Slight Blunting of Leading Edge of an Immersed Body on the Flow around it at Hypersonic Speeds," TT F-35, 1960, NASA.

[3]Hayes, W. D. and Probestein, R. F., "Hypersonic Flow Theory," *Inviscid Flows*, Vol. I, Academic Press, New York, 1966, p. 364.

[4]Schnieder, W., "Asymptotic Behavior of Hypersonic Flow over Blunted Slender Wedges," *AIAA Journal*, Vol. 6, No. 11, Nov. 1968, pp. 2235–2236.

[5]Stollery, J. L., "Hypersonic Viscous Interaction on Curved Surfaces," *Journal of Fluid Mechanics*, Vol. 43, Pt. 3, 1970, pp. 497–511.

[6]Stollery, J. L., Pimputkar, S., and Bates, L., "Hypersonic Viscous Interaction," *Fluid Dynamic Transactions*, Vol. 6, Pt. II, 1971, pp. 545–562.

[7]Murthy, A. V., "Studies in Hypersonic Viscous Interactions," Ph.D. thesis, Dec. 1972, Dept. of Aerodynamics, Cranfield Institute of Technology, Bedford, England.

[8]Kemp, J. H., "Hypersonic Viscous Interaction on Sharp and Blunt Inclined Flat Plates," *AIAA Journal*, Vol. 7, No. 7, July 1969, pp. 1280–1289.

[9]Cheng, H. K. and Kirsch, J. W., "On the Gas Dynamics of an Intense Explosion with an Expanding Contact Surface," *Journal of Fluid Mechanics*, Vol. 39, Pt. 2, 1969, pp. 289–305.

Subsonic Flow into a Downstream Facing Inlet

Theo G. Keith Jr.*
The University of Toledo, Toledo, Ohio

BY changing the direction on the internal engine flow, through the use of a variable pitch fan, reverse thrust can be generated in a fan engine. However, in accomplishing a thrust reversal by this method, flow will be taken into the propulsor from its downstream opening and thus the exhaust nozzle will function as an inlet. Since the nozzle was not necessarily intended to be used in this fashion, it is of interest to examine expected performance characteristics. As a first step, a simple extension of an earlier study by Fradenburg and Wyatt, Ref. 1, is used in this note to estimate the total pressure recovery of the inlet as a function of the freestream Mach number for parametric values of the inlet or duct Mach number.

The flow model assumes that the nozzle can be represented as a sharp-lip cylindrical duct facing in the downstream direction, and that the internal duct flow is separated due to the fact that the flow cannot turn the 180° required to stay attached to the duct wall. Because of this, the total pressure does not remain constant throughout the flow field.

Since the analysis closely follows that presented in Ref. 1, only the major points will be brought out herein. A mass-momentum balance on a control volume drawn around the inlet results in the following two expressions:

Received January 14, 1974. This work was performed while the author was an ASEE summer faculty fellow at the NASA Lewis Research Center.

Index categories: Aircraft Deceleration Systems; Subsonic and Transonic Flow.

*Assistant Professor, Dept. of Mechanical Engineering. Member AIAA.